

# Selecting the AERONET data.

## Part I: Substantiation of the techniques

Yu.Ya. Matyushchenko,<sup>1</sup> V.K. Oshlakov,<sup>2</sup> and V.E. Pavlov<sup>1</sup>

<sup>1</sup> *Institute of Water and Ecological Problems,  
Siberian Branch of the Russian Academy of Sciences, Barnaul*

<sup>2</sup> *Institute of Atmospheric Optics,  
Siberian Branch of the Russian Academy of Sciences, Tomsk*

Received July 19, 2005

Theoretical calculations of intensity of scattered light and observations of absolute phase functions of brightness in the clear-sky atmosphere are used as a basis to propose methods for selecting data of monitoring measurements of sky brightness, presented at AERONET sites, aimed at eliminating cloudy situations. The methods are based on the following condition. Scattering of solar light in the clear-sky atmosphere occurs on the system of particles of a wide size spectrum what excludes the manifestations of lobe structure of the scattering phase function. A number of CIMEL photometer sites of brightness observations, located in deserts, woodlands, oceanic islands, and Russian cities, use the selection of observation data to eliminate cloudy situations. Small percentage of clear-sky days has been recorded in the oceans.

It is well known that qualitative information on column aerosol optical characteristics can be obtained from analysis of spectral transmission, intensity of scattered light, and some other characteristics of the clear-sky atmosphere.<sup>1</sup> Recently, NASA has deployed CIMEL photometers for ground-based monitoring of aerosol optical depth and daytime sky brightness in solar almucantar at many sites over the globe; it provides abundant observation material usable for construction of both regional and global models of atmospheric aerosol. However, the tabular values of sky brightness, available from AERONET site,<sup>2</sup> do not exclude completely the effect of clouds.

Three-level data selection, made mainly by NASA specialists to exclude cloud effects, covers the situations when clouds in the sky are located along the direction towards the Sun. However, in most of the cases the brightness of separate cloud systems enter into the final series of sky-brightness data denoted as Level-2. Therefore, each researcher, who uses AERONET information for one or another purpose, is forced to solve this problem.<sup>3-7</sup> Most objective way of excluding cloud effect from analyzed series seems to be through inclusion of satellite information, not always available for a number of reasons. In this regard, it is necessary to substantiate and represent compactly such methods of analysis of angular distributions of observed sky brightness, which would deliberately exclude cloud situations from the subsequent consideration. This task for solar almucantar is solved in the present study.

Main physical prerequisite used in all developments below is that in the majority of cases, the aerosol scattering in the entire atmosphere occurs on the systems of particle of wide size spectrum. Using the representations from Ref. 8 as a starting point, we shall assume aerosol particles to be presented by

three fractions: ultramicroscopic (Aitken nuclei), submicron, and the coarse fraction. Within each fraction, the particle size-distribution function is logarithmically normal. For instance, it can be shown<sup>9</sup> that the mean aerosol scattering phase function  $f_a(\varphi)$  at the wavelength  $\lambda = 0.55 \mu\text{m}$ , obtained through inversion of experimental data on sky brightness in south-eastern Kazakhstan,<sup>10</sup> in the interval of scattering angles  $2^\circ \leq \varphi \leq 160^\circ$  is approximated by a sum of scattering phase functions, corresponding to the above-mentioned fractions, accurate within a few percent. Parameters of the size modes are as follows:  $\sigma^2 = 0.4$  and  $a = -0.1$  (ultramicroscopic fraction, 15%), 0.4 and 0.4 (submicron fraction, 60%), and 0.4 and 0.8 (coarse fraction, 25%). Here,  $\sigma$  is the variance of logarithms of radii,  $a = -\ln \rho_0$ ;  $\rho_0 = 2\pi r_0/\lambda$ ; and  $r_0$  is the mean geometric radius of spherical particles. Numbers in parentheses indicate the contributions of each fraction to the total aerosol extinction. Refraction index is 1.5; aerosol absorption is negligibly small (coefficient of imaginary part of the refraction index  $\eta$  is assumed to be equal to zero).

It should be noted that the above-mentioned range of scattering angles for solar almucantar  $2^\circ \leq \varphi \leq 160^\circ$  covers all the AERONET observation data. The aerosol scattering phase function  $f_a(\varphi)$ , summed over all fractions, has a minimum near  $\varphi = 120^\circ$  (we shall denote this angle by  $\varphi_{\min}$ ); and as  $\varphi$  varies from  $120^\circ$  to near solar aureole ( $2^\circ$ ) and from  $\varphi = 120^\circ$  to  $\varphi = 160^\circ$ , i.e., in the backward direction, the scattering phase function represents two systematically increasing "pieces" of functions, supported, e.g., by analysis of tabulated data.<sup>11</sup> The lobe structure, typical for separate large particles and media with narrow particle size distribution, is absent for these values of parameters  $\rho_0$  and  $\sigma$  in the interval of scattering angles  $2^\circ \leq \varphi \leq 160^\circ$ .

Combining the weights of the above-mentioned fractions in different proportions in the total aerosol extinction (or parameters  $\lambda$ ,  $\sigma$ ,  $\rho_0$ ,  $n$ , and  $\eta$ ), it is possible to substantially change the shape of the aerosol scattering phase function  $f_a(\varphi)$ , mimicking its natural variations. For instance, by varying the contributions of the fractions to the optical scattering depth, the asymmetry coefficient of scattered fluxes for aerosol particles

$$\Gamma_a = \frac{\int_{\frac{\pi}{2}}^{\pi} f_a(\varphi) \sin \varphi d\varphi}{\int_{\frac{\pi}{2}}^{\pi} f_a(\varphi) \sin \varphi d\varphi} \quad (1)$$

in this case will range from 5.6 (for pure ultramicroscopic fraction) to 15.7 (for pure coarse fraction). This range of  $\Gamma_a$  variations, in essence, includes the absolute majority of natural realizations of the asymmetry coefficient.

The observed absolute scattering phase function  $f(\varphi)$  contains, in addition to aerosol component  $f_a(\varphi)$ , the molecular single scattering component  $f_m(\varphi)$ , as well as the components of multiple scattering  $f_2(\varphi)$  and reflection from the underlying surface  $f_q(\varphi)$  with albedo  $q$  (Ref. 1):

$$f(\varphi) = f_a(\varphi) + f_m(\varphi) + f_2(\varphi) + f_q(\varphi); \quad (2)$$

therefore, in using the observed total function  $f(\varphi)$  for selection of AERONET data, one should realize that each its component can influence the angular brightness distribution. Obviously, when  $f_a(\varphi)$  is summed with  $f_m(\varphi)$ , because of the weak angular dependence of the latter,  $(1 + \cos^2\varphi)$ , will substantially decrease the elongation of the single scattering phase function  $f_1(\varphi) = f_a(\varphi) + f_m(\varphi)$  as compared with the pure aerosol scattering phase function  $f_a(\varphi)$ . At the same time, depending on wavelength, turbidity of the atmosphere, and type of the aerosol scattering phase function, the position of the minimum in angular brightness distribution in single-scattering case will markedly change:  $\varphi_{\min}$  may shift from  $120^\circ$  to  $90^\circ$  angle, inclusive. However, the condition of systematic  $f_1(\varphi)$  growth for  $\varphi < \varphi_{\min}$  in direction of smaller angles and for  $\varphi > \varphi_{\min}$  in direction of larger angles will remain unchanged.

Specialists in theory of radiative transfer assume the surface reflection to be Lambertian and, correspondingly, the component  $f_q$  to be independent of the scattering angle. Therefore, we shall assume that its addition to  $f_1(\varphi)$  will not influence the systematic increase of brightness with the decrease of  $\varphi$  from  $\varphi_{\min}$  and with the increase of  $\varphi$  at angular distances  $\varphi > \varphi_{\min}$ . As to the multiple scattering component  $f_2(\varphi)$ , compared to scattering phase function of the initial scattering  $f_1(\varphi)$ , it usually is a weakly forward elongated function with insignificant

angular dependence in the backward hemisphere.<sup>12</sup> Thus, it is quite reasonable to suppose that the total scattering phase function  $f(\varphi)$  will be steadily increasing function for smaller angles at  $\varphi < \varphi_{\min}$  and for larger scattering angles at  $\varphi > \varphi_{\min}$ . Analysis of absolute scattering phase functions  $f(\varphi)$ , calculated by Zhuravleva<sup>13</sup> for a large number of atmospheric parameters, completely confirmed this proposition.

Thus, from the radiative transfer theory it follows that for aerosol particles of a wide size spectrum, the observed function  $f(\varphi)$  must systematically grow as  $\varphi$  varies leftward and rightwards of  $\varphi_{\min}$ . If in the practice there occur distortions of this growth in the form of jumps at some angles or within intervals of angles, they most probably will be not due to the effects of the scattering phase function but rather due to horizontal inhomogeneities in the spatial distribution of scattering particles in the atmosphere and primarily due to the presence of separate clouds in the sky. Of course, this criterion of selection of clear-sky situations must be checked using reliable experimental material under idealized cloud-free conditions.

Such observation time series of absolute scattering phase functions  $f(\varphi)$  were previously obtained at the Astrophysical Institute of Academy of Sciences of Kazakh Soviet Socialist Republic and Kazakh Pedagogical Institute. In the south-eastern Kazakhstan, the observation sites were at the Astrophysical Observatory and Kirbaltabai village; in Black Sea coast of Caucasus it was Gelendzhik.<sup>14</sup> In addition to  $f(\varphi)$  observations, the narrow-angle photometers of daytime sky were used to measure the optical depths  $\tau$  and control the stability of atmospheric optical properties in time according to the method of Pyaskovskaya-Fesenkova.<sup>15</sup> The photometers were equipped with narrow-band interference filters centered at the wavelengths 0.40, 0.45, 0.55, 0.67, 0.71, 0.87, and 1.02  $\mu\text{m}$ ; that is, they corresponded to the spectral range in which AERONET data are presented. Scattering phase functions were measured with the step  $\Delta\varphi = 2^\circ$  for scattering angles  $2^\circ \leq \varphi \leq 10^\circ$ , then with the step  $\Delta\varphi = 5^\circ$  for  $10^\circ \leq \varphi \leq 20^\circ$ , with step  $\Delta\varphi = 10^\circ$  for  $20^\circ \leq \varphi \leq 60^\circ$ , and then with the step  $\Delta\varphi = 20^\circ$  until the maximum scattering angle  $\varphi_{\max}$  determined from the condition

$$\cos\varphi = \cos^2 Z + \sin^2 Z \cos\Psi, \quad (3)$$

where  $Z$  is solar zenith angle;  $\Psi$  is azimuth of observed point of the sky measured from the direction towards the Sun. At the point  $\Psi = 180^\circ$  we have:  $\varphi_{\max} = 2Z$ . Since sky brightness observations presented in AERONET are performed for  $Z$  values not exceeding  $70\text{--}75^\circ$ , the  $\varphi_{\max}$  value in the limiting case reaches  $140\text{--}150^\circ$ . The experimental data obtained in the south-eastern Kazakhstan and in Gelendzhik precisely for these  $Z$  (and the corresponding  $\varphi_{\max}$  values), were used to explore the regularity of  $f(\varphi)$  increase on either side of  $\varphi_{\min}$ . As an example, Figure 1 shows scattering phase functions for  $\varphi \geq 60^\circ$ , measured

in Kirbaltabai on days with maximum and minimum atmospheric turbidity. Aerosol optical depths on these days were correspondingly 0.06 and 0.34 at  $\lambda_1$  and 0.05 and 0.32 at  $\lambda_2$ .

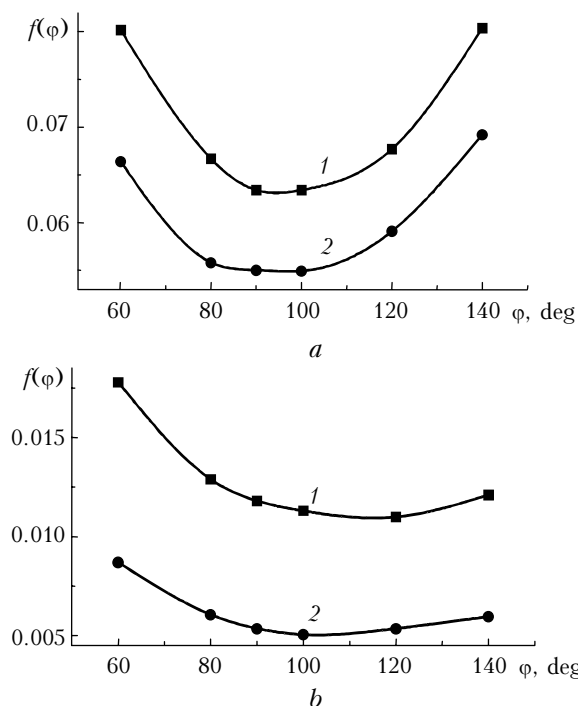


Fig. 1. Scattering phase functions  $f(\varphi)$  for scattering angles 60–140° according to measurements in Kirbaltabai for wavelengths  $\lambda_1 = 0.405 \mu\text{m}$  (a) and  $\lambda_2 = 0.706 \mu\text{m}$  (b) for high (line 1) and low (line 2) atmospheric turbidity.

The error of  $f(\varphi)$  measurement in relative units (which are just required in solving this problem) is about 1% at the confidence probability 0.95. From Fig. 1 it is seen that the angle  $\varphi_{\text{min}}$  can be determined quite reliably accurate within a few degrees. Sometimes in the red and infrared regions of the spectrum, the minimum of function  $f(\varphi)$  is not strictly fixed, lying in the angular interval  $\Delta\varphi = 10\text{--}30^\circ$ , so inside the interval there may occur  $f(\varphi)$  fluctuations, usually in the range 1–2%. In these cases, the brightness regularly increases with variation of  $\varphi$  on both sides from the boundaries of this preselected interval. Quite analogous conclusion can be drawn from analysis of experimental data in different parts of the spectrum on other clear days.

We have studied more than 150 scattering phase functions, measured at 16 scattering angles. The position of the  $\varphi_{\text{min}}$  can be judged from observation data presented in Table 1.

Table 1. Number of cases (in %) of location of angle  $\varphi_{\text{min}}$  at one of the three angular distances in the solar almucantar

$\varphi_{\text{min}}, \text{deg}$	$\lambda, \mu\text{m}$				
	0.45	0.65	0.70	0.85	1.01
90	13	5	2	0	0
100	87	80	72	41	22
120	0	15	26	59	78

As expected, the role of the components  $f_m(\varphi)$  and  $f_2(\varphi)$  in forming the shape of observed scattering phase function  $f(\varphi)$  increases, as the wavelength decreases, thus shifting  $\varphi_{\text{min}}$  toward smaller angles. For all the observed scattering phase functions, there was always true that  $f(\varphi)$  increased with systematic change of  $\varphi$  on both sides of  $\varphi_{\text{min}}$ .

To make sure that this condition can be used in analysis of AERONET data not only under field conditions but also for the urban atmosphere, we have considered the experimental time series of aerosol single scattering phase functions observed in the near-ground air layer in Alma-Ata.<sup>16</sup> The absolute scattering phase functions of this type are additively summed up with absolute scattering phase functions of overlying layers and determine the sky brightness over the city. Their inspection has shown that the condition of decrease of  $f_a(\varphi)$  from small angles to  $\varphi_{\text{min}}$  and increase of  $f(\varphi)$  past  $\varphi_{\text{min}}$  is fulfilled for all 45 scattering phase functions studied at different wavelengths in the visible spectral range.

Thus, summarizing the previously mentioned, it is reasonable to propose that in the clear-sky atmosphere this condition must be practically always satisfied, and so it can serve a basis for sampling clear-sky realizations for solar almucantar in the system of AERONET data. In the case of a cloud within the photometer field of view along some of the viewing directions ( $\varphi + \Delta\varphi$ ), it is highly probable that cloud brightness will be larger than the brightness of the clear-sky atmosphere at angular distance  $\varphi$  from the Sun (we mean observations for  $\varphi < \varphi_{\text{min}}$ ). As a consequence, there will be a stepwise change of the smooth angular behavior of  $f(\varphi)$ . Cloud presence can be detected especially reliably at large angular distances from the Sun for  $\varphi > 70\text{--}80^\circ$ , where brightness of the clear-sky atmosphere depends weakly on the scattering angle. Low-contrast clouds, present in solar almucantar for  $\varphi < 60\text{--}70^\circ$ , with brightness insignificantly exceeding the brightness of the clear sky, are very difficult to detect with this criterion.

To exclude situations characterized by the presence of these low-level systems, we can propose a more stringent criterion of selection of AERONET data. From the analysis of observations, performed in south-eastern Kazakhstan and Gelendzhik, it was found that for all points of the studied experimental arrays (2400 directions  $\varphi$ ), with exception of 16, the following formulas are valid:

$$f(\varphi) - f(\varphi + \Delta\varphi) > f(\varphi + \Delta\varphi) - f(\varphi + 2\Delta\varphi) \text{ for } \varphi < \varphi_{\text{min}} \quad (4)$$

and

$$f(\varphi + \Delta\varphi) - f(\varphi) < f(\varphi + 2\Delta\varphi) - f(\varphi + \Delta\varphi) \text{ for } \varphi > \varphi_{\text{min}}, \quad (5)$$

where the step  $\Delta\varphi$  is specified in correspondence with gradient of brightness variations (see discussion above). Examples of angular dependences of logarithms of the differences  $[f(\varphi) - f(\varphi + 10^\circ)]$  in the range  $10^\circ \leq \varphi \leq 90^\circ$  are presented in Fig. 2, while for the region of aureole  $[f(\varphi) - f(\varphi + 2^\circ)]$  in the range  $2^\circ \leq \varphi \leq 10^\circ$  in Fig. 3. Same absolute scattering phase

functions as in Fig. 1 are considered. We can clearly see systematic increase of the differences  $[f(\varphi) - f(\varphi + \Delta\varphi)]$  with the decrease of the scattering angle  $\varphi$ .

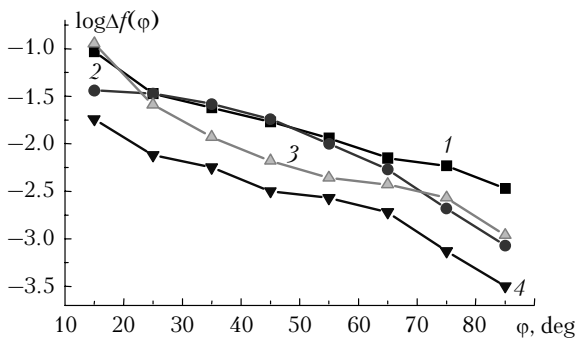


**Fig. 2.** Logarithms of the differences  $\log\Delta f(\varphi)$  for scattering angles 10–90° according to measurements in Kirbaltabai for wavelengths  $\lambda = 0.706$  (curves 1 and 2) and  $0.405 \mu\text{m}$  (curves 3 and 4) for high (curves 1 and 3) and low (curves 2 and 4) atmospheric turbidity.

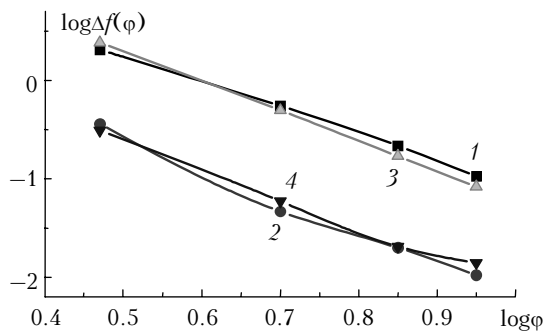


**Fig. 3.** Logarithms of differences  $\log\Delta f(\varphi)$  for scattering angles 3–9° according to measurement in Kirbaltabai for wavelengths  $\lambda = 0.706$  (curves 1 and 2) and  $0.405 \mu\text{m}$  (curves 3 and 4) for high (curves 1 and 3) and low (curves 2 and 4) atmospheric turbidity.

It should be noted that the deviations from formulas (4) and (5), mentioned above, are not related to wavelength and solar zenith angle, and that only three of them took place in the forward hemisphere, that is for scattering angles  $\varphi < 90^\circ$ . In the near-ground layer of Alma-Ata, for these same  $\varphi$ , we recorded five cases of deviation out of 45 considered. In other words, formula (4) for near-ground layer holds at least in 90% of situations. Therefore, this formula can be used as an additional “stringent” criterion in choosing cloud-free situations according to AERONET data. This criterion is most efficient in the forward hemisphere of the sky.

It should be noted that the use of “stringent” criterion, i.e., formulas (4) and (5), as compared with a less stringent one of systematic growth of  $f(\varphi)$  with variation of  $\varphi$  on both sides of  $\varphi_{\min}$ , leads to reduction of the number of cases passed the test, by about 2 to 3 times for deserts, 5 to 10 times for continental forests, and by 10 to 20 times for ocean islands. These figures apply to the cases to be considered below.

Another necessary condition in selection of experimental data with the purpose of their subsequent objective analysis is establishment of the fact of

uniform distribution of atmospheric turbidity along horizontal directions within the errors of optical measurements. This issue has been already considered in some earlier papers such as Refs. 5 and 17. If aerosol in each layer of the stratified atmosphere is horizontally uniform, the optical characteristics of the right and left halves of the sky, conventionally divided by the plane of the solar vertical, must be identical. In this case, independent of the altitude distribution of turbidity, the following condition must be met for the sky brightness in the solar almucantar

$$B(\Psi) = B(360^\circ - \Psi) \quad (6)$$

for  $\Psi$  varying from 0 to 180° (brightness measurements for CIMEL photometers start at  $\Psi \geq 2^\circ$ ).

Here, it is necessary to note that, when it is required to pass from azimuthal dependence of the sky brightness  $B(\Psi)$  or  $B(360^\circ - \Psi)$  to angular dependence  $B(\varphi)$ , formula (3) should be used. In its turn,  $B(\varphi)$  and absolute scattering phase function  $f(\varphi)$  are related by the formula

$$B(\varphi) = E_0 m f(\varphi) \exp(-\tau m), \quad (7)$$

where  $E_0$  is the spectral solar constant;  $m$  is the atmospheric mass along the direction toward the Sun, and  $\tau$  is the total atmospheric optical depth.<sup>15</sup> All data, required for the passage, can be found in AERONET tables, in explicit or implicit form. It is also worthy to note that, by virtue of fulfillment of formula (3), the  $\Psi$  values in the region of aureole  $\varphi < 10^\circ$  differ little from  $\varphi$  (somewhat exceed it), provided that solar zenith angle  $Z$  is no less than  $60^\circ$ .

In order to use the condition (6) in analysis of AERONET data, it is necessary to evaluate initial accuracy with which it is fulfilled. It is well known that the accuracy of sky brightness measurements with CIMEL photometers is about 5% in absolute values.<sup>18</sup> This estimate determines the possibilities of all subsequent manipulations with data on the observed brightness  $B(\Psi)$  and  $B(360^\circ - \Psi)$  for determination of aerosol single scattering phase function  $f_a(\varphi)$ , separation of the aerosol optical depth into absorption and scattering components, or solution of some other radiation problems. If differences between  $B(\Psi)$  and  $B(360^\circ - \Psi)$  do not exceed 5%, these observations can be used in the above cases.

In contrast to Ref. 6, which uses 21 azimuth directions to estimate uniformity of turbidity distribution, here we shall assume that condition (6) should hold for all azimuth angles with the accuracy no worse than 5%. However, preliminary examination of sky brightness at small angular distances from the Sun, that is for azimuths 2–2.5 and 358–356.5°, in AERONET tables has shown that the differences between them always exceed 5%. Very often, NASA specialists denote brightness in circumsolar directions through “–100”, meaning they are 100% uncertain. They appear either to the left or to the right of the solar disk during four-fold automatic scans of the zone of circumsolar aureole by CIMEL photometer in each observation series.

For instance, in Dalanzadgad, Mongolia, none out of 8800 available brightness distributions, is free of “-100” instances for the above-indicated  $\Psi$  values. In Ascension Island, Atlantic, the number of distributions is 40 000, and only in 1/10 of these cases “-100” readings are absent. This by no means implies that in the sky near the Sun, either on one or the other side clouds constantly appear and disappear.

Unlikely, this observation result follows from errors of photometry of the aureole. Most probably, this is because of irregular and uncontrolled appearance of flashes of direct solar light in the entrance photometer channel during its not very precise mechanical pointing to the above-indicated regions of the sky near the sun disk. This issue needs further study; so we shall use in our analysis the data of observations of sky brightness for azimuths larger than 3 and smaller than 357°.

We shall selectively examine the results of brightness measurements in AERONET to see if they simultaneously meet “stringent” conditions (4), (5), and (6) and for all directions in the solar almucantar. For this, we choose three locations in the arid zone: (1) Solar Village, Arabian Peninsula, (2) Tinga Tingana, Australia, and (3) Dalanzadgad, Mongolia; three islands: (1) Thaiti (Central Pacific), (2) Nauru (West Pacific), and (3) Ascension Island, North Atlantic; at three continental forested locations: (1) Belterra (South America), (2) Santa-Cruz, North America, and (3) Zambezi, Africa; as well as at three Russian cities: Moscow, Tomsk, and Barnaul. All brightness survived preliminary selection in NASA are classified as Level-2 data. Table 2 presents the data for four wavelengths  $\lambda$ ; entries are total number of considered angular brightness distributions  $N$ , number of cases when conditions (3), (4), and (5)

are met, as well as the values  $\delta = (n/N) \cdot 100\%$ . Note that when conditions (4), (5), and (6) are applied separately, the second condition produces more serious data reduction: by a factor of 2 to 10, depending on observation point.

These tabular data require serious considerations. In addition to the well known fact that the contrast of local aerosol and, moreover, cloud system in the atmosphere against the background of clear sky sharpen with the increase of wavelength,<sup>19,20</sup> they contain the following information. The number of situations which, upon fulfillment of conditions (4), (5), and (6), are considered as clear-sky ones with uniform aerosol distribution in horizontal is negligible. Even in desert on Arabian peninsula in the blue region of the spectrum, it does not exceed 3% (in IR region it is two times smaller). Moreover, in cities the observation data usable for analysis are absent at all.

Here it is necessary to note the following. Starting from publications of Pyaskovskaya-Fesenkova in early 1940s,<sup>15</sup> all subsequent 50-year experience of studying optical parameters of the clear-sky atmosphere at the Astrophysical Institute of Kazakh Academy of Sciences point out to a different thing. In mountains and, especially, in steppes and semi-deserts, absolutely clear days have been recorded not that seldom when the difference between  $B(\Psi)$  and  $B(360^\circ - \Psi)$  occurred to be no more than 1–3% at the angular distances  $\varphi \geq 10^\circ$ . The clear-sky situations are most frequent in fall periods. Good convergence of brightness to the left and to the right of the solar disk (usually divergence is less than 3% and, of course, it is always no more than 5%) is observed in circumsolar aureole  $2^\circ \leq \varphi \leq 10^\circ$ , provided, of course, that optical finder is used to point the small-angle photometer to the given point of aureole.

**Table 2. Fulfillment of the conditions (4), (5), and (6) in a number of locations over the globe for azimuths  $3^\circ \leq \Psi \leq 357^\circ$**

$\lambda, \mu\text{m}$	$N$	$n$	$\delta$	$N$	$n$	$\delta$	$N$	$n$	$\delta$
	1. Solar Village			2. Tinga Tingana			3. Dalanzadgad		
1.02	14457	237	1.6	3672	15	0.4	2361	2	0.1
0.87	14390	221	1.5	3663	11	0.3	2252	0	0
0.68	14311	182	1.3	3653	17	0.5	2126	1	0
0.44	14329	427	3.0	3656	25	0.7	2063	5	0.2
	4. Thaiti			5. Nauru			6. Ascension Island		
1.02	4305	0	0	8405	0	0	9983	1	0
0.87	4325	1	0	8398	0	0	9862	2	0
0.68	4317	1	0	8350	1	0	9834	7	0.1
0.44	4289	0	0	8305	4	0	9776	19	0.2
	7. Belterra			8. Santa-Cruz			9. Zambezi		
1.02	8552	1	0	2701	1	0	1368	15	1.1
0.87	8566	0	0	2676	2	0.1	1359	22	1.6
0.68	8520	5	0.1	2657	1	0	1327	35	2.6
0.44	8489	19	0.2	2678	4	0.1	1318	31	2.4
	10. Moscow			11. Tomsk			12. Barnaul		
1.02	1250	0	0	1295	0	0	306	0	0
0.87	1249	2	0.2	1289	0	0	307	0	0
0.68	1247	7	0.6	1317	0	0	310	0	0
0.44	1246	5	0.4	1320	0	0	314	0	0

**Table 3. Fulfillment of conditions (4), (5), and (6) (values of  $\delta^*$  in %) in a number of locations over the globe for azimuths  $10^\circ \leq \Psi \leq 350^\circ$** 

$\lambda, \mu\text{m}$	Observation site number (see Table 2)											
	1	2	3	4	5	6	7	8	9	10	11	12
1.02	12.7	6.1	1.4	0.1	0.0	0.6	0.1	0.2	8.6	1.8	3.1	2.0
0.87	13.7	10.5	1.6	0.1	0.1	0.8	0.2	0.3	11.3	3.4	4.5	3.3
0.68	16.4	16.8	3.2	0.4	0.2	1.9	0.6	0.6	15.1	7.1	5.8	5.2
0.44	20.7	21.7	7.4	0.9	0.9	4.7	1.8	2.2	13.6	13.2	10.2	8.9

This observation method was implemented in the practice in as early as beginning of 1960s.<sup>21</sup> CIMEL photometers have no optical finder, and mechanical pointing of the instrument to the points of aureole, lying symmetrically to the left and to the right of the Sun, seemingly does not ensure 5% accuracy in matching the brightness values  $B(\Psi)$  and  $B(360^\circ - \Psi)$ . Moreover, the absolute imprecision of pointing is individual for each concrete observation series, impeding introduction of average correction factors into the entire data array. Since the sky brightness near the Sun has large gradient over wide range of angles  $\Psi$ , significant differences between  $B(\Psi)$  and  $B(360^\circ - \Psi)$  due to imprecise pointing of photometer take place not only for azimuths 2–2.5 and 358–357.5°, but also in the entire region of circumsolar aureole, i.e., for  $10^\circ \leq \varphi$ . In this case, if criterion (6) is straightforwardly used in practice, there will appear an illusion that large particles have spatially nonuniform distribution in the atmosphere on different sides of the plane of solar vertical.

However, even if certain corrections are not introduced to the AERONET data on aureoles, and to use brightness values averaged over four readouts, in each observation series, nonetheless these  $B(\Psi)$  distributions can be used to solve a certain class of radiation problems. This is, e.g., the problem of determination of aerosol scattering optical depths from sky brightness. For its solution one can use the integrals<sup>9,13</sup>:

$$\Delta_1 = 2\pi \int_0^{\frac{\pi}{2}} f(\varphi) \sin \varphi d\varphi \quad (8)$$

and

$$\Delta = 2\pi \int_0^{\pi} f(\varphi) \sin \varphi d\varphi. \quad (9)$$

Because of large weight of sine in the integrands and narrow range of the scattering angles 0–10°, when mechanically averaged observation data are used for aureole, the errors of measurements of circumsolar aureole for  $3^\circ \leq \varphi \leq 10^\circ$  will have little effect on the accuracy of evaluating the integrals.<sup>22</sup>

Moreover, using some empirical formulas for determination of brightness at small scattering angles,<sup>1,21</sup> and assuming that the precision of pointing of photometer to the points of aureole is systematic in each complete series of observations of angular brightness distribution, we can try to reconstruct the actual angular dependence of  $f(\varphi)$ . This task is

planned to be solved in the near future. Now, let us determine the quantity  $\delta^*$ , characterizing the difference between the brightness  $B(\Psi)$  and  $B(360^\circ - \Psi)$  for  $\Psi \geq 10^\circ$ , that is by excluding circumsolar aureole completely from analysis (Table 3).

From comparison of Tables 2 and 3 it follows that exclusion of zone of aureole from selection criterion (6) leads to obvious increase of the number of the cases suitable for further analysis. In particular, in arid sites in Arabian peninsula and in Australia it reaches 10–20%. Owing to this fact, the information on absorptance of arid particles, obtained from observations by the method from Ref. 23, can be provided with a good statistics.<sup>24</sup>

However, at some observation sites the number of clear-sky situations, with aerosol uniformly distributed in horizontal directions, is still very small. On ocean islands in the spectral region  $\lambda \geq 0.68 \mu\text{m}$ , it does not exceed 1%. Thus, now the question is on agenda: are the data, obtained on so rare clear days on ocean islands, sufficiently representative to be used for construction of aerosol models of the atmosphere over ocean?

## References

1. A.I. Ivanov, G.Sh. Livshits, V.E. Pavlov, B.T. Tashenov, and Ya.A. Teifel, *Scattering of Light in the Atmosphere* (Nauka, Alma-Ata, 1968), Part 2, 116 pp.
2. <http://aeronet.gsfc.nasa.gov>.
3. M. Hess, P. Koepke, and I. Schult, *Bull. Amer. Meteorol. Soc.* **79**, 831–844 (1998).
4. A. Smirnov, B.N. Holben, T.F. Eck, O. Dubovik, and I. Slutsker, *Remote Sensing & Environ.*, No. 73, 337–349 (2000).
5. O. Dubovik and M.D. King, *J. Geophys. Res. D* **105**, No. 16, 20673–20696 (2000).
6. O. Dubovik, B.N. Holben, T.F. Eck, A. Smirnov, Y.J. Kaufman, M.D. King, D. Tanre, and I. Slutsker, *J. Atmos. Sci.* **59**, 590–608 (2002).
7. N.N. Ulyumdzhieva, N.E. Chubarova, and A.V. Smirnov, *Meteorol. Gidrol.*, No. 1, 48–57 (2005).
8. G.V. Rozenberg, G.I. Gorchakov, Yu.S. Georgievskii, and Yu.S. Lyubovtseva, in: *Atmospheric Physics and Climate Problems* (Nauka, Moscow, 1980), 262 pp.
9. T.Z. Muldashev, V.E. Pavlov, and Ya.A. Teifel, *Atm. Opt.* **2**, No. 11, 959–963 (1989).
10. V.S. Antyufeev, A.I. Ivanov, G.Sh. Livshits, and G.A. Mikhailov, *Izv. Akad. Nauk SSSR, Fiz. Atmos. Okeana* **16**, No. 2, 146–155 (1980).
11. E.G. Yanovitskii and Z.O. Dumanskii, *Tables for Light Scattering by Polydisperse System of Spherical Particles* (Naukova Dumka, Kiev, 1972), 123 pp.
12. A.V. Pavlov, V.E. Pavlov, and T.Z. Muldashev, *Atmos. Oceanic Opt.* **9**, No. 5, 438–441 (1996).

13. V.E. Pavlov, V.V. Pashnev, A.S. Shestukhin, and T.B. Zhuravleva, *Vychislitelnye Tekhnologii* **7**, No. 4 (32), 34–41 (2002).
14. V.N. Glushko, A.I. Ivanov, G.Sh. Livshits, V.E. Pavlov, and I.A. Fedulin, *Brightness and Polarization of the Clear-sky Atmosphere* (Nauka, Alma-Ata, 1979), 201 pp.
15. E.V. Pyaskovskaya-Fesenkova, *Study of Light Scattering in the Earth's Atmosphere* (Izd. Akademii Nauk SSSR, Moscow, 1957), 219 pp.
16. T.P. Toropova, A.P. Ten, G.V. Bushueva, and O.D. Tokarev, in: *Extinction of Light in the Earth's Atmosphere* (Nauka, Alma-Ata, 1976), pp. 33–113.
17. Yu.Ya. Matyushchenko and V.E. Pavlov, in: *Proceedings of Interregional Ecological Forum* (Barnaul, 2004), pp. 138–141.
18. B.N. Holben, T.F. Eck, I. Slutsker, D. Tanre, J.P. Buis, A. Setzer, F. Vermote, J.A. Reagan, Y.J. Kaufman, T. Nakajima, F. Lavenu, I. Jankoviak, and A. Smirnov, *Remote Sensing & Environ.*, No. 66, 1–16 (1998).
19. V.P. Galileyskii, A.M. Morozov, and V.K. Oshlakov, *Atm. Opt.* **3**, No. 11, 1116–1118 (1990).
20. V.K. Oshlakov, *Atm. Opt.* **3**, No. 4, 392–396 (1990).
21. T.P. Toropova and B.E. Pavlov, in: *Proceedings of Third All-Union Scientific Meteorological Conference* (Gidrometeoizdat, Leningrad, 1964), Vol. 6, pp. 122–130.
22. T.Z. Muldashev, V.E. Pavlov, and Ya.A. Teyfel, *Izv. Akad. Nauk SSSR, Fiz. Atmos. Okeana* **27**, No. 8, 831–841 (1991).
23. T.B. Zhuravleva, V.E. Pavlov, V.V. Pashnev, and A.S. Shestukhin, *J. Quant. Spectrosc. Radiat. Transfer* **88**, 191–209 (2004).
24. A.S. Shestukhin, “*Integral and nephelometric methods of determination of aerosol scattering optical depth from measurements of sky brightness*,” Author's Abstract of Cand. Phys.-Math. Sci. Dissert. Barnaul (2003), 19 pp.